Magnetic Resonance Imaging Exploration of the Human Brain During 10 kHz Spinal Cord Stimulation for Failed Back Surgery Syndrome: A Resting State Functional Magnetic Resonance Imaging Study

Sander De Groote, PT*; Lisa Goudman, PT*†; Ronald Peeters, PhD‡; Bengt Linderoth, MD, PhD§; Peter Vanschuerbeek, MSc, PhD¶; Stefan Sunaert, MD, PhD‡; Mats De Jaeger, PT*; Ann De Smedt, MD, PhD**; Maarten Moens, MD, PhD*¶†† (ID)

Introduction: Apart from the clinical efficacy of high frequency spinal cord stimulation at 10 kHz, the underlying mechanism of action remains unclear. In parallel with spinal or segmental theories, supraspinal hypotheses have been recently proposed. In order to unveil hidden altered brain connectome patterns, a resting state functional magnetic resonance imaging (rsfMRI) protocol was performed in subjects routinely treated for back and/or leg pain with high-frequency spinal cord stimulation (HF-SCS) HF-SCS at 10 kHz.

Methods: RsfMRI imaging was obtained from ten patients with failed back surgery syndrome who were eligible for HF-SCS at 10 kHz. Specifically-chosen regions of interest with different connectivity networks have been investigated over time. Baseline measurements were compared with measurements after 1 month and 3 months of HF-SCS at 10 kHz. Additionally, clinical parameters on pain intensity, central sensitization, pain catastrophizing, and sleep quality were correlated with the functional connectivity strengths.

Results: The study results demonstrate an increased connectivity over time between the anterior insula (affective salience network) and regions of the frontoparietal network and the central executive network. After 3 months of HF-SCS, the increased strength in functional connectivity between the left dorsolateral prefrontal cortex and the right anterior insula was significantly correlated with the minimum clinically important difference (MCID) value of the Pittsburgh sleep quality index.

Conclusion: These findings support the hypothesis that HF-SCS at 10 kHz might influence the salience network and therefore also the emotional awareness of pain.

Keywords: Spinal cord stimulation, failed back surgery syndrome, magnetic resonance imaging, mechanisms of action, chronic pain

Conflict of Interest: Maarten Moens has received speaker fees from Medtronic and Nevro Corp. The remaining authors have no conflicts of interest to report.

INTRODUCTION

Since the day that high frequency spinal cord stimulation (HF-SCS) at 10 kHz has been introduced as therapeutic option for failed back surgery syndrome (FBSS), the general thinking of *how to stimulate the spinal cord* has changed. This is not only due to its clinical superiority against traditional SCS, but also by the paradigm of stimulating the spinal cord without generating paresthesias (1–3). Despite its effectiveness, the exact working mechanism of HF-SCS at 10 kHz is still unclear. Both spinal and supraspinal mechanisms are hypothetically involved in the overall effectiveness of this therapeutic modality (4). Aside from causing segmental effects, it has been suggested that traditional, paresthesia-generating, SCS induces several changes in modulation circuits located in the cerebrum and brainstem. An inhibitory effect of traditional SCS on somatosensory evoked potentials, and potential mediators like the thalamus and

Address correspondence to: Maarten Moens, MD, PhD, Universitair Ziekenhuis Brussel (UZ Brussel), Laarbeeklaan 101, 1090 Brussels, Belgium. Email: maarten.moens@uzbrussel.be

* Department of Neurosurgery, Universitair Ziekenhuis Brussel, Brussels, Belgium;
† Department of Physiotherapy, Human Physiology and Anatomy, Faculty of Physical Education & Physiotherapy, Vrije Universiteit Brussel, Brussel, Belgium;
‡ Department of Radiology, Universitair Ziekenhuis Leuven, UZ, Leuven, Belgium;
§ Department of Clinical Neuroscience, Karolinska Institute, Stockholm, Sweden;
¶ Department of Radiology, Universitair Ziekenhuis Brussel, Brussels, Belgium;
** Department of Neurology, Universitair Ziekenhuis Brussel, Brussels, Belgium; and
†† Center for Neurosciences (C4N), Vrije Universiteit Brussel (VUB), Brussels, Belgium

the anterior cingulate cortex (ACC), could play a role in the mechanism of action (MOA) of SCS as well (5–8).

To investigate the MOA of SCS in human cerebral circuits, different neuroimaging techniques (e.g., MR Spectroscopy [MRS], single photon emission computerized tomography [SPECT], positron emission tomography [PET], electroencephalography [EEG], and functional magnetic resonance imaging [fMRI]) are able to capture alterations in modulation circuits (6–10). fMRI is especially interesting due to the robustness and test–retest reliability of the functional connectivity (FC) method in clinical applications (11,12). It has been shown in a recent systematic review about rsfMRI that patients with chronic back pain have an elevated activation in the medial prefrontal cortex (mPFC), cingulate cortex, amygdala, insula, and sensory motor integration regions together with a disrupted default mode network (13). Additionally, a recent work by Kolesar et al. (2017) demonstrated that a chronic pain state in patients with FBSS influences the connectivity of several resting state networks such as the salience, central executive, and sensorimotor network (14). However, in patients with FBSS, no research on the mid-term and long-term influences of HF-SCS at 10 kHz on the resting state networks has been published. It is of crucial importance to explain the influence of SCS on the functional connectivity during a steady state treatment period.

To address this gap of research into the underlying mechanisms of action of this paresthesia-free therapy in patients with FBSS, our objectives were twofold:

1. To identify alterations in FC in resting-state networks in patients with FBSS, treated with HF-SCS at 10 kHz.
2. To observe whether there is an association between clinical data and functional brain changes in patients with FBSS, treated with HF-SCS at 10 kHz.

MATERIAL AND METHODS

Participants

Ten consecutive patients, diagnosed with FBSS, and eligible to HF-SCS at 10 kHz, were recruited at the University Hospital Brussels between September 2015 and May 2017 (15). All participants provided written informed consent prior to participation. The study was approved by the ethics committee of the University Hospital Brussels (B.U.N. 143201526931) and registered at ClinicalTrials.gov (NCT02650362). This study was conducted according to the revised declaration of Helsinki (1998).

Study Protocol

This exploratory, prospective study consisted of six individual visits (Fig. 1). The first (V1), third (V3), and fifth (V5) visit were short appointments of about 20 minutes and were scheduled 2 weeks before the neuro-imaging visits (V2, V4, V6). During visits V1, V3, and V5, every subject received an Actiwatch spectrum plus (Phillips Respironics Inc., Murrysville, PA, USA) in order to collect objective sleep quality data and a numeric rating scale (NRS) diary for pain intensity. During V2 (baseline), V4 (1 month after permanent HF-SCS: T1) and V6 (3 months after permanent HF-SCS: T2) patients were asked to complete three questionnaires (Pain Catastrophizing Scale [PCS], Pittsburgh sleep quality index [PSQI], central sensitization index [CSI]) and they underwent a neuroimaging fMRI-protocol. Between the second and third visit, patients underwent a trial implantation of SCS, followed by a definitive implantation of the SCS system. All patients received two percutaneous leads. Two percutaneous leads were placed in the posterior spinal epidural space under radiographic imaging and attached to either an external stimulator (during the trial phase) or a subcutaneously implanted pulse generator (IPG). For HF10 therapy, the distal tip of one lead was placed at T8, whereas a second lead tip was placed at T9, both near anatomical midline. Stimulation was configured bipolarly in all patients. Accordingly, to the Belgian reimbursement rules (trial period of 4 weeks and pain reduction of 50%), all ten patients included in this study were implanted with a Senza rechargeable system (Nevro Corp., Redwood City, CA, USA). The stimulation parameters of the permanent IPG remained constant during the whole protocol.

MRI Data Acquisition

The first two MRI scans of the first two recruited subjects were performed on a Philips Achieva 3 T Intera MRI scanner using a transmit-receive head coil. Total acquisition time for each MRI session is 8 min 20 sec. Anatomical images were acquired using a T1-weighted gradient echo pulse sequence (3D T1-TFE scan), consisting of 60 axial slices with slice thickness = 1.0 and no inter-slice gap, TR = 7.74 ms, TE = 3.75 ms, flip angle = 8°, scan matrix = 240 x 240 x 60 and field of view (FOV) = 240 x 240 x 60 mm^3. Functional imaging data were acquired with a spin echo echo-planar imaging (SE-EPI) consisting of 250 volumes of 24 axial slices covering the whole brain, with a slice thickness of 4 mm and gap of 1 mm, TR = 2 s, TE = 55 ms, flip angle = 90°, matrix size = 96 x 94 and FOV = 230 x 230 mm^2.

All the other MRI scans were performed on a GE MR 750w Discovery 3 T using a 24-channel head coil. A high-resolution anatomical image was acquired using an axial fast spoiled gradient echo (FSPGR) bravo scan, consisting of 124 axial slices with slice thickness 1 mm, no inter-slice gap, TR = 7.74 ms, TE = 3.75 ms, flip angle = 12°, scan matrix = 256 x 256 and FOV = 240 x 240 mm^2.
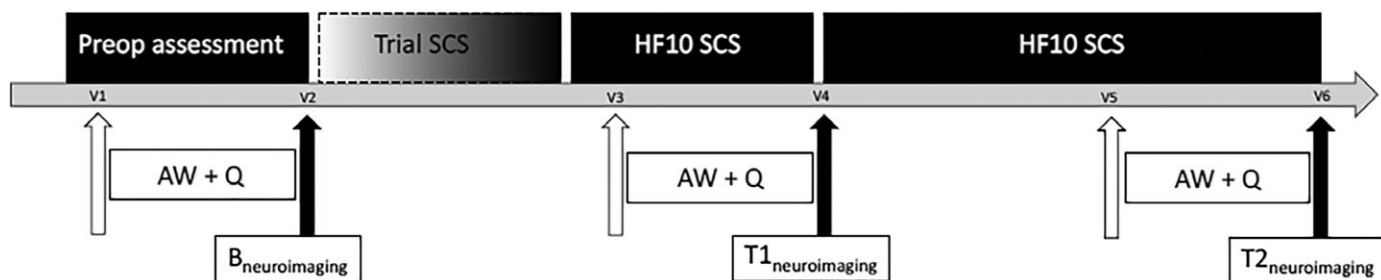

Figure 1. Study protocol. Patients with FBSS were enrolled 1 month before SCS trial implantation and were followed-up for 3 months after permanent implantation. Every patient underwent a neuroimaging protocol at baseline, 1 month after SCS and 3 months after SCS. SCS, spinal cord stimulation; HF-10 SCS, high frequency spinal cord stimulation; AW, actiwatch; Q, questionnaires; B, baseline; T1, 1 month of HF10-SCS; T2, 3 months of HF-10 SCS; V, visit.
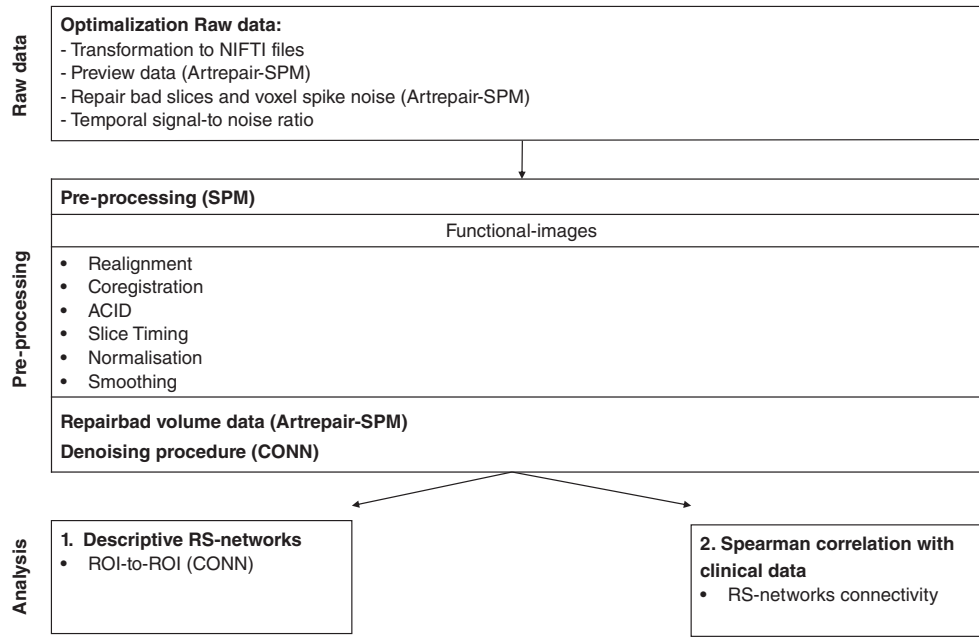
Optimalization Raw data:
- Transformation to NIFTI files
- Preview data (Artrepair-SPM)
- Repair bad slices and voxel spike noise (Artrepair-SPM)
- Temporal signal-to noise ratio

Raw data

Pre-processing (SPM)

Functional-images

- Realignment
- Coregistration
- ACID
- Slice Timing
- Normalisation
- Smoothing

Repairbad volume data (Artrepair-SPM)
Denoising procedure (CONN)

Pre-processing

1. Descriptive RS-networks
- ROI-to-ROI (CONN)

2. Spearman correlation with clinical data
- RS-networks connectivity

Analysis

Figure 2. Data processing algorithm. All data were preprocessed after optimalization of the raw data. After preprocessing, a ROI-to-ROI analysis and correlation analysis with clinical data were performed. NIFTI, neuroimaging informatics technology initiative; SPM, statistical parametric mapping; ACID, artifact correction in diffusion MRI; CONN, functional connectivity toolbox for Matlab; RS, resting state; ROI, regions of interest.

Functional imaging data consisted of 250 rsfMRI volumes using a spin echo echo-planar imaging sequence. The following scan parameters were selected: 23 axial slices covering the whole brain with slice thickness of 4 mm and a 1 mm inter-slice gap, TR = 2 sec, TE = 55 ms, flip angle = 90°, matrix size = 128 x 128 and FOV = 240 x 240 mm^2. Patients were instructed to stay awake and to immediately inform the investigators in case any unusual sensation was felt at the implantation site, because the SCS was left on during imaging.

Imaging Processing

Resting State fMRI Preprocessing and Data Analysis

The resting state fMRI data were pre-processed and analyzed using Statistical Parametric Mapping (SPM) software version 12 (Fig. 2) (Wellcome Trust Center for Neuroimaging; http://www.fil.ion.ucl.ac.uk/spm/) and a functional connectivity toolbox (CONN, version 17.C, MATLAB-based cross-platform software, freely available from NITRC at https://www.nitrc.org/projects/conn). First, all data were transformed to NIFTI files and previewed with ArtRepair (see https://www.nitrc.org/projects/art_repair/) to detect the global mean intensity and motion outliers in fMRI data. Additionally, ArtRepair detected and repaired bad slices (slices with artifacts due to radiofrequency [RF]-coil fluctuations) in the raw images, whereby the default threshold (outslice = 18) was selected.

Blood oxygen level-dependent (BOLD) fMRI time series preprocessing steps included the removal of the first three volumes for signal stabilization, realignment to remove movement artifacts, and HySCO 2.0 (using Artifact correction in diffusion MRI [ACID] toolbox) for hyperelastic susceptibility artifact correction of diffusion weighted images. In addition, phase swap (PS) fMRI series were co-registered to the mean of the functional time series. Furthermore, differences in acquisition time between slices were corrected, the fMRI series were normalized using normalization parameters of the co-registered anatomical scan and normalized

image volumes were smoothed using a Gaussian kernel with a FWHM of 8 mm. Subsequently, outlier volumes were repaired with Artrepair. Therefore, the default threshold of 1.5% variation in standard deviation away from the global brain activation mean as a function of time and a default threshold at 0.5 mm/TR variation were selected. Finally, the temporal signal-to-noise ratio (tSNR), in which the mean signal over time is taken into account, was used to determine the SNR of fMRI time series. After performing the resting state fMRI preprocessing, an age-covariate was added. During the normalization step of the preprocessing protocol, the MRI data were transformed into a common 3D brain space (MNI space).

Subsequently, denoising procedure in CONN included 1) linear regression of CSF and WM following the Compor method; 2) linear regression of the six motion realignment parameters; 3) identification and interpolation of inconsistent frames due to time courses and movement time courses; 4) bandpass filtering between 0.008 and 0.09 Hz. To avoid the introduction of false negative correlations, the global signal was not regressed out (16,17). To assess region of interest (ROI)-ROI functional connectivity matrices, the Pearson correlation coefficient between the mean signal intensity BOLD time courses within all ROI-pairs of each network was calculated with CONN. A Fisher's r-to-z transformation was being applied to each correlation map to allow statistical group-level analysis (18). Subsequently, a second-level analysis was performed using a paired *t*-test to identify coherent functional connectivity patterns of paired ROIs between two conditions (B vs. T1, B vs. T2, T1 vs. T2) in patients with covariate age. We corrected for multiple comparisons by limiting the false discovery rate to 5% (19).

ROI Identification

Extraction of default mode network (DMN), sensorimotor network (SMN), salience network (SALN), frontoparietal network (FPN), central executive network (CEN), and cerebellar network (CN) consisted of average BOLD signal time series within the ROI voxels, calculated in CONN. ROIs of each network, except CEN,

Table 1. Region of Interest Identification.

Network	BA	Region	x, y, z	Abbreviation
Default mode network	10	Medial prefrontal cortex	1, 55, −3	MPFC
	19	Left lateral parietal cortex	−39, −77 33	LPL
	39	Right lateral parietal cortex	47, −67, 29	LPR
	7	Posterior cingulate cortex	1, −61, 38	PCC
Sensorimotor network	4	Left sensorimotor cortex	−55, −12, 29	LSMC
	4	Right sensorimotor cortex	56, −10, 29	RSMC
	6	Paracentral lobule	0, −31, 67	PCL
Salience network	32	Anterior cingulate cortex	0, 22, 35	ACC
	13	Left anterior insula	−44, 13, 1	LAI
	47	Right anterior insula	47, 14, 0	RAI
	9	Left rostral prefrontal cortex	−32, 45, 27	LRPFC
	9	Right rostral prefrontal cortex	32, 46, 27	RRPFC
	40	Left supramarginal gyrus	−60, −39, 31	LSMG
	40	Right supramarginal gyrus	62, −35, 32	RSMG
Frontoparietal network	9	Left lateral prefrontal cortex	−43, 33, 28	LLPFC
	40	Left inferior parietal cortex	−46, −58, 49	LIPC
	9	Right lateral prefrontal cortex	41, 38, 30	RLPFC
	40	Right inferior parietal cortex	52, −52, 45	RIPC
Central executive network	9	Right dorsolateral prefrontal cortex	43, 22, 34	RDLPFC
	9	Left dorsolateral prefrontal cortex	−43, 22, 34	LDLPFC
	40	Right inferior parietal lobule	51, −47, 42	RIPL
	40	Left inferior parietal lobule	−51, −51, 36	LIPL
Cerebellar network		Cerebellar posterior network	0, −79, −32	CP
		Cerebellar anterior network	0, −63, −30	CA

The x, y, and z montreal neurological institute peak coordinates of each region of interest are provided (in millimeter).
BA, Brodmann area.

were already pre-programmed in CONN with a spherical radius of 10 mm, using the FSL Harvard-Oxford Atlas. CEN was predefined, based on the article of Fair et al. (20) (Table 1).

Statistical Analysis

Statistical analyses were performed using the statistical package for the social sciences software (IBM SPSS for Windows, version 25, SPSS Inc., Chicago, Illinois, USA). Due to the small sample size ($N = 10$), non-parametric tests were used. Friedman tests with post-hoc Wilcoxon tests were calculated to analyze differences in FC and differences in questionnaires, between the three visits.

To calculate the correlation between FC and clinical questionnaires, the differences in relative scores on the questionnaires and the absolute connectivity values of ROI/ROI analyses between all timepoints were used. Besides questionnaires with statistically significant differences in scores over time, also minimum clinically important difference (MCID) and clinical cut-off values were used in this correlation analysis. For NRS and PSQI scores, MCID values (NRS: ≥ 2 points difference and PSQI: ≥ 3 points of difference) were considered (21–23). For the PCS and the CSI questionnaire cut-off scores (PCS: ≤ 30 and CSI: ≤ 40) were considered (24,25). Relative differences between B and T1 were calculated as ((B-T1)/B) * 100. Similar calculations were performed for the differences between B-T2. A Simes procedure was applied to correct for multiple testing. The null-hypothesis is rejected if $P_{(j)} \leq j \frac{\alpha}{n}$ for any j = 1,2,…,n with $P_1,…,P_n$ the ordered p values and $\alpha = 0.05$ (26).

All patients were compliant with the neuroimaging protocols. Missing data in the questionnaires (CSI = 20%, AW = 10%, PCS = 3.3%, NRS-diary = 3.3%) was imputed with the multiple imputation technique whereby five imputations were used.

RESULTS

Patient Characteristics

A total of ten right-handed subjects with FBSS (eight females, two males) and median age of 56 y (Q1:50,8-Q3:57), were included in this study (Table 2). All subjects reported predominant back pain (back pain: median NRS 5.9 [Q1:4.9-Q3:6.8]; leg pain: median NRS 5.2 [Q1:3.7-Q3:6.4]). The mean duration of the pain syndrome prior to SCS implantation was 4.2 years with a maximum of 14 years. All subjects underwent, per definition, at least once spinal surgery, however, five underwent multiple surgeries (>2). Nine subjects experienced a neuropathic component (scored at least 4/10 on douleur neuropathique 4 [DN4] questionnaires). All but one subject used (weak) opioids on a regular basis, in combination with pregabalin. All ten patients responded successfully to the trial of 4 weeks and reported a pain reduction during that period of more than 50%. Subsequently, they received a permanent Senza rechargeable system (Nevro Corp., Redwood City, CA, USA). Regarding the stimulation parameters, a pulse width of 30 μ sec was used in combination with a frequency of 10, 000 Hz and amplitudes between 1,5 and 2,5 mA. The variation of amplitudes was defined based on an algorithm. This algorithm starts with a rigid protocol varying from 0 to 3,5 mA and starting with 2,5 mA. The patient has the liberty to change the amplitude with steps of 0,5 mA in function of individual pain relief.

Clinical Results

There was a significant difference in total score of the PCS ($p = 0,033$), PSQI ($p = 0,042$) and NRS-back ($p = 0,008$) between the three time points (baseline, 1 month of SCS and 3 months of SCS) (Fig. 3).

Table 2. Individual Patient Characteristics.

Patient	Sex	Age	Pain duration (years)	Previous surgeries	Pain medication pre-SCS	DN4 score
1	M	57	14	3	Weak opioids + pregabaline	6
2	F	56	5	2	Weak opioids + pregabaline	4
3	F	67	1	1	Weak opioids + pregabaline	5
4	M	57	1	1	Weak opioids + pregabaline	6
5	F	46	5	3	Weak opioids + pregabaline	4
6	F	53	3	1	Weak opioids + pregabaline	5
7	F	46	3	1	Weak opioids + pregabaline	8
8	F	56	3	2	None	5
9	F	59	6	5	Weak opioids + pregabaline	2
10	F	50	1	1	Weak opioids + pregabaline	8

Individual patient characteristics of the 10 included patients before SCS implantation.
F, female; M, male.

Catastrophizing

At baseline, the median reported PCS-total was 31.5 (Q1:19.5-Q3:41.25) as compared to 16 (Q1:12.5 -Q3:25) at T1 and 28.5 (Q1:14-Q3:37.75) at T2. There was a significant improvement (49.2%) in the PCS score from baseline towards T1 ($p = 0.01$). Regarding the different subscales of the PCS, only magnification reveals a significant reduction (61.8%) at T1 as compared to baseline ($p = 0.01$).

At Baseline, five of ten patients reached the threshold of 30 on the PCS. Two of them still had significant levels of catastrophizing after 1 month of SCS. However, after 3 months of SCS, again five patients demonstrated high levels of catastrophizing (27).

Sleep Quality

No significant differences were observed after monitoring objective sleep parameters (sleep onset latency, actual sleep percentage, wake-after-sleep onset, number of wake bouts, mean night-time activity, fragmentation-index and sleep efficiency) with the Actiwatch spectrum plus between the three time points (data was averaged over the last 2 weeks before neuroimaging). Regarding subjective sleep quality with the PSQI, a significant reduction (23.1%) was measured between T2 (median PSQI = 10 [Q1:7.25-Q3:14]) and baseline (median PSQI = 13 [Q1:11-Q3:15]) ($p = 0.05$).

Using the MCID on the PSQI (≥3points of difference between two time points), after 1 month of SCS, 40% of the patients improved and after 3 months of SCS, this proportion further increased up to 60% (22).

Pain Intensity

At baseline, the median NRS-back was 5.9 (Q1:4.9-Q3:6.8), at T1 4.2 (Q1:3.2-Q3:4.3), and at T2 3.1 (Q1:2.7-Q3:4). A significant reduction was observed between baseline and T1 (28.7%; $p = 0.02$), as well as between baseline and T2 (46.7%; $p = 0.01$). No significant improvements in leg pain were found (median NRS at baseline: 5.2 [Q1:3.7-Q3:6.4], at T1: 3.4 [Q1:2.4-Q3:5.3], at T2: 4.1 [Q1:3.5-Q3:4.9], $p = 0.097$).

Applying the MCID of two points of ten, after 1 month of stimulation, 70% (20%) of patients improved for back (leg) pain. After 3 months of stimulation, 80% (30%) of patients improved for back (leg) pain (21,28,29).

Central Sensitization

The CSI scores showed no significant differences compared to baseline (median CSI = 46 [Q1:40.75-Q3:49.75]) after neither 1 month of stimulation (CSI = 46 [Q1:37.75-Q3:55.5]); $p = 0.83$), nor after 3 months of SCS (CSI = 47 (Q1:32.25-Q3:58.75); $p = 0.88$).

Utilizing cut-off values of 40, at baseline and at T1, 70% of patients experienced symptoms of central sensitization. After 3 months of SCS, only 60% reached the threshold (24).
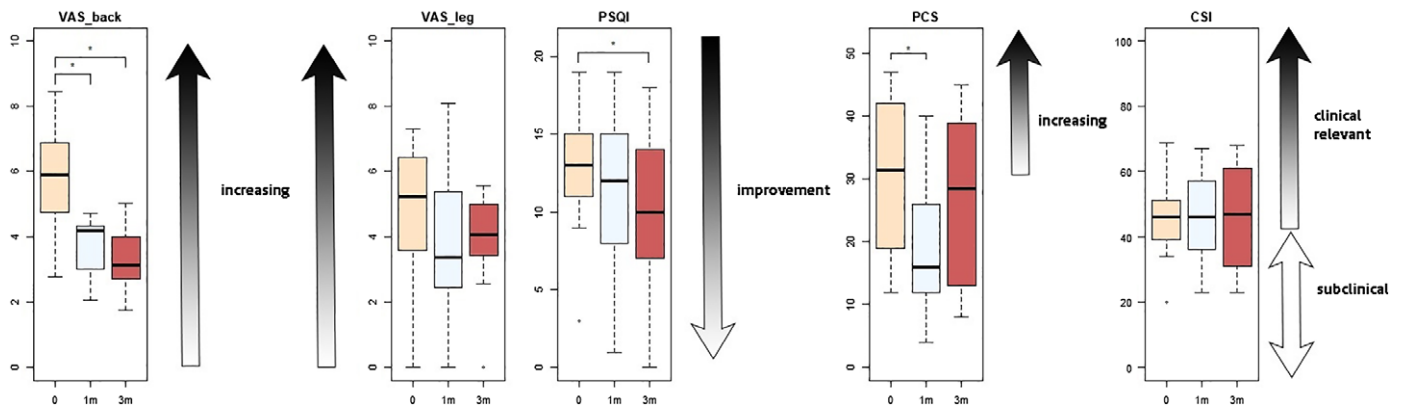

Figure 3. Boxplots of the clinical results of NRS, PSQI, CSI, and PCS scores of all patients. Pink, blue, and red boxes are representing respectively baseline data, data after 1 month of SCS and data after 3 months of SCS. Gray arrows indicate the diagnostic criteria. Black horizontal lines represents median scores of each questionnaire. *$p < 0.05$. VAS, visual analogue scale; PSQI, Pittsburg sleep quality index; PCS, pain catastrophizing scale; CSI, central sensitization index. [Color figure can be viewed at wileyonlinelibrary.com]

Functional Connectivity Results

Connectivity strength matrices between all ROI-pairs were calculated at baseline, T1 and T2. Subsequently, a comparison of FC differences between baseline-T1 and baseline-T2 was calculated as a connectivity strength matrix and visualized on a 3D anatomical template (Fig. 4).

Significant increases ($p < 0.05$ FDR corrected) in connectivity strength between LLPFC and RAI, and between RLPFC and LSMC, after 1-month SCS (T1) in comparison with baseline were found (Fig. 4a). The matrix between baseline and T2 revealed a significant increase ($p < 0.05$ FDR corrected) in connectivity strength between LDLPFC-RAI, LAI-LIPC, RAI-LIPC, and ACC-CP after 3 months SCS (T2) in comparison with baseline. A significant decrease in connectivity strength after 3 months SCS (T2) in comparison with baseline was found in ROI-pair PCL-RLPFC (Fig. 4b). Remarkably, ROI-pairs that were significantly altered after T1, were not withheld at T2 and vice versa. However, an uncorrected significant increase in ROI-pair ACC-CP was already present after 1-month SCS ($p < 0.01$).

When evaluating individual differences in effect size of FC strength (Fig. 5) after 1-month SCS, an increase in FC strength was assessed in ten patients at T1 and seven subjects at T2 for RAI-LPFC, ten at the T1 and four at T2 for LSMC-RLPFC. An increase in effect size was observed in six subjects at T1 and ten subjects at T2 for LDLPFC-RAI, five at the T1 and nine at T2 for LAI-LIPC, seven at T1 and ten at T2 for RAI-LIPC and ten at T1 and nine at T2 for ACC-CP. For ROI-pair PCL-RLPFC, a decrease of FC-strength after 1-month HF-SCS at 10 kHz was found in seven subjects. After 3 months of HF-SCS at 10 kHz a decrease became visible, which was present in nine subjects.

Correlation Between Functional Connectivity and Clinical Results

As mentioned above, only the PSQI total, PCS total, and the NRS back scores were statistically significant more than the three measurements time points and were considered for the correlation analysis with the functional connectivity ROI-ROI pairs ($p < 0.05$ FDR corrected). Only a significant correlation was found between the RAI-LLPFC connectivity and the total PCS score ($p = 0.048$, R = 0.636). However, this correlation failed to pass the procedure for multiple testing.

Correlation results between functional connectivity ROI-ROI pairs and clinical questionnaires, taking into account the MCID and the clinical cut-off scores, revealed significant correlations between the LDLPFC-RAI connectivity and the total PCS score ($p = 0.04$, R = 0.9) and the PSQI score ($p = 0.02$, R = 0.89) at T2. Additionally, a significant correlation was found between the PCL-RLPFC ROI-pair and the total PSQI score ($p = 0.019$, R = −0.89) at T2. Of all the reported statistically significant correlations, only the correlation between the LDLPFC-RAI ROI-pair and the total score of the PSQI passed the procedure for multiple testing.

DISCUSSION

Although the reported clinical superiority of HF-SCS at 10 kHz therapy over conventional SCS, several "working hypotheses" trying to explain the mechanism of action of HF-SCS at 10 kHz have been proposed (1,2,30–43). The thread that links them all is the putative segmental mechanism, not (largely) based on the Gate Control Concept (4). This study is the first report of the use of resting state fMRI during HF-SCS at 10 kHz stimulation in patients with FBSS to explore (in) direct supraspinal effects of this type of SCS.

Most of the statistically significant changes were found between baseline and 3 months of HF-SCS at 10 kHz. An in-depth analysis of the FC results at 1 month showed no statistically significant changes. However, a non-significant trend toward the 3 months results could already be noticed. The connectivity between the RAI and LLPFC seems to increase over time, but due to a large variability at 3 months HF-SCS at 10 kHz, this trend was not significant. From the results of the functional connectivity analysis during HF-SCS at 10 kHz, it appears that the affective salience network has a crucial role to play. This study showed an increased connectivity over time between the anterior insula region involved in emotional awareness (44) and regions from the frontoparietal network (lateral prefrontal cortex and inferior parietal cortex), involved in attention and working memory (45). The frontoparietal network has been recognized as a key player in expectancy-induced modulation of pain (45). One remarkable aspect from these results is the increased strength of connection over time (1 month vs. 3 months of HF-SCS) and this statement was valid for almost every subject. Although a strong correlation has not been found, the same trend can be detected in the clinical data. Patients statistically improved over time regarding pain relief for the back-pain component and subjective sleep quality.

The right anterior insula connects also with increasing strength to the dorsolateral prefrontal cortex, which is one of the key regions of the central executive network. This result is in line with other studies on chronic pain patients, where the right anterior insula, as the main causal output within the salience network, projects to the central executive network (46–48). After 3 months of HF-SCS, the increased strength in FC was also significantly correlated with the MCID value of the PSQI. Recently, a study revealed a positive association between longer sleep duration and functional connectivity between the anterior insula and dorsolateral prefrontal cortex (49). Therefore, we hypothesize that ROI-pair LDLPFC-RAI might be a possible biomarker to monitor improvements in sleep quality. To explore the possible role of biomarker, further specifically designed studies are needed.

The relation between the right anterior insula and the posterior part of the cerebellum remains unclear, despite the increasing strength of connectivity during HF-SCS at 10 kHz, although the cerebellum is known to have an active role in acute and chronic pain (50). In relation with SCS, the anterior insula or in general the affective salience network, seems to be very active making connections with other networks related to pain (51,52). Furthermore, in opioid research, the anterior insula was also allocated as an important brain region related to the alteration of the affective dimension of pain (53). Similar with the work of Deogaonkar et al., which investigated the functional connectivity between on and off state of conventional SCS in a mixed population, the influence of the limbic system seems to play a crucial role in the treatment effect of SCS (19). This could lead to the hypothesis that HF-SCS at 10 kHz might influence the salience network and therefore also the medial pain pathway, a hypothesis on which burst SCS has been working on for several years (8,54). Recently, De Ridder et al. suggested that HF-SCS at 10 kHz and burst stimulation could have the same underlying mechanism by modulating the medial pain pathway (55). Previous work reported similar effects on the medial pain pathway in conventional SCS, which indicates that these findings for paresthesia-free stimulation cannot be exclusive for Burst SCS (6,7).

Besides the transparent analysis scheme and the consistency in statistical analysis, this study also has some limitations. It may be difficult to directly compare the clinical effects in our study to previous studies because of the different outcome parameters: visual analogue scale versus NRS, outpatient time stamp pain intensity
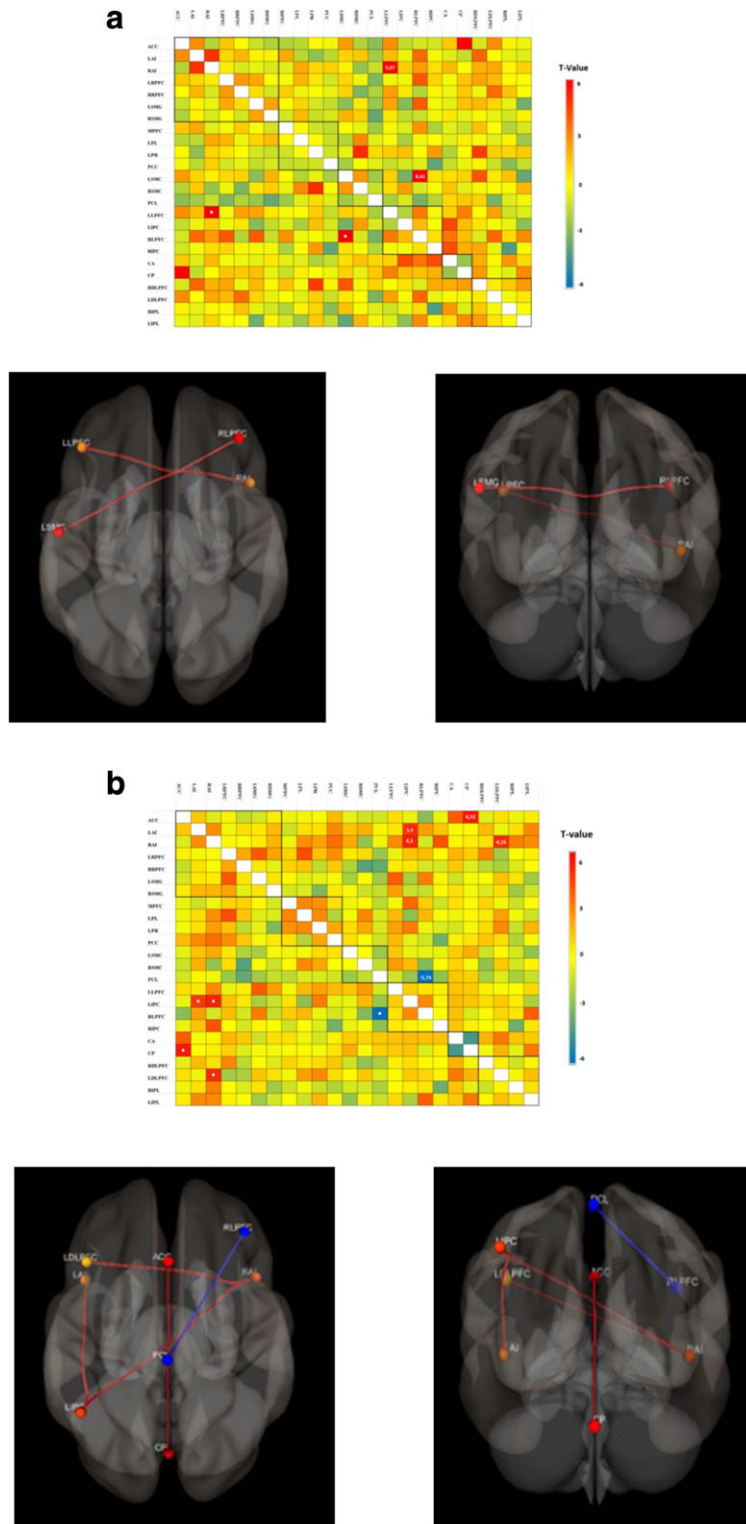
Figure 4. ROI-ROI matrices, visualization of functional connectivity in resting state networks. Differences of the functional connectivity strength in ROI-ROI pairs between treatment session T1 (a) versus baseline and T2 (b) versus baseline in all ten patients are shown in the ROI-ROI matrices. The significant results ($p < 0.05$ FDR corrected) were visualized by colored circles projected on a 3D anatomical brain template (superior/posterior view). The red lines indicate increased connectivity after T1(a)/T2(b) versus baseline while blue lines indicate decreased connectivity, and their thickness varies as a function of the associated T-value. In the ROI-ROI matrices, the color scale represents the T-value of connectivity strength between two brain regions (ROIs) of the selected resting state networks. Blue colors indicate a negative decreased connectivity while the red colors indicate a positive increased connectivity between two ROIs. Significant connectivity links are symbolized with a white dot and their coherent T-value. LLPFC, left lateral prefrontal cortex; RAI, right anterior insula; LSMC, left sensorimotor cortex; RLPFC, right lateral prefrontal cortex; LDLPFC, left dorsolateral prefrontal cortex; LAI, left anterior insula; LIPC, left inferior parietal cortex; ACC, anterior cingulate cortex; CP, cerebellar posterior network; PCL, paracentral lobule; T1, 1 month SCS; T2, 3 months SCS. [Color figure can be viewed at wileyonlinelibrary.com]
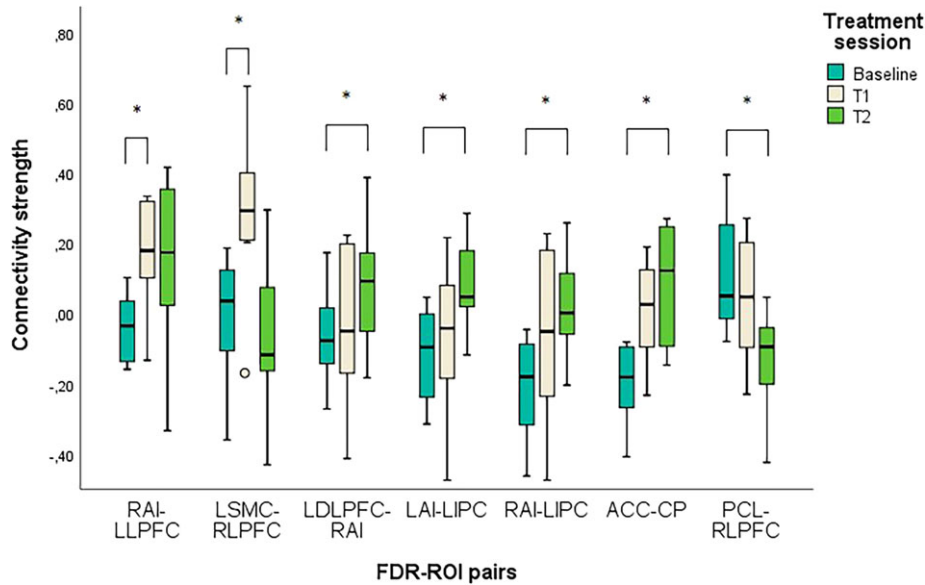
Figure 5. Effect size of functional connectivity (FC) in FDR-ROI pairs at baseline, T1, and T2. Representing significant ROI-pairs in functional connectivity strength after T1 or T2. Mean results of FC strength provide an increase after 1 month in RAI-LLPFC and LSMC-RLPFC ROI-pair. After T2, there is a significant increase in 4 FDR-ROI pairs (LDLPFC-RAI, LAI-LIPC, RAI-LIPC, ACC-CP) and a decrease at PCL-RLPFC. LLPFC, left lateral prefrontal cortex; RAI, right anterior insula; LSMC, left sensorimotor cortex; RLPFC, right lateral prefrontal cortex; LDLPFC, left dorsolateral prefrontal cortex; LAI, left anterior insula; LIPC, left inferior parietal cortex; ACC, anterior cingulate cortex; CP, cerebellar posterior network; PCL, paracentral lobule; T1, 1 month SCS; T2, 3 months SCS. *Alteration of FC at T1/T2 in comparison with ($p < 0.05$ FDR corrected). [Color figure can be viewed at wileyonlinelibrary.com]

versus pain intensity diary and mean versus median pain intensity reporting. Additionally, we only had a limited sample size with an uneven sex distribution in this explorative study, for which we need to be very precautious with making inferences. Finally, except from the poor temporal resolution, the functional networks are also sensitive to pharmacological manipulations, a factor difficult to control in chronic pain patients. During the preprocessing of the data, no additional corrections were made for potential physiological noise.

CONCLUSION

Summing up, this resting state fMRI study revealed for the first time that HF-SCS at 10 kHz in patients with FBSS changes the functional connectivity in specific regions of the salience, frontoparietal and central executive network. The anterior part of the insula seems to play a crucial role in these changes. These findings may suggest a role of the medial pathway as integrator for pain relief by HF-SCS at 10 kHz.

Acknowledgements

Authorship Statement

REFERENCES

1. Kapural L, Yu C, Doust MW et al. Novel 10-kHz high-frequency therapy (HF10 therapy) is superior to traditional low-frequency spinal cord stimulation for the treatment of chronic Back and leg pain: the SENZA-RCT randomized controlled trial. *Anesthesiology* 2015;123:851–860.
2. Kapural L, Yu C, Doust MW et al. Comparison of 10-kHz high-frequency and traditional low-frequency spinal cord stimulation for the treatment of chronic Back and leg pain: 24-month results from a multicenter, randomized, controlled pivotal trial. *Neurosurgery* 2016;79:667–677.
3. Tiede J, Brown L, Gekht G, Vallejo R, Yearwood T, Morgan D. Novel spinal cord stimulation parameters in patients with predominant back pain. *Neuromodulation* 2013;16:370–375.

8

4. Linderoth B, Foreman RD. Conventional and novel spinal stimulation algorithms: hypothetical mechanisms of action and comments on outcomes. *Neuromodulation* 2017;20:525–533.

5. Bentley LD, Duarte RV, Furlong PL, Ashford RL, Raphael JH. Brain activity modifications following spinal cord stimulation for chronic neuropathic pain: A systematic review. *Eur J Pain* 2016;20:499–511.

6. Moens M, Marien P, Brouns R et al. Spinal cord stimulation modulates cerebral neurobiology: a proton magnetic resonance spectroscopy study. *Neuroradiology* 2013;55:1039–1047.

7. Moens M, Sunaert S, Marien P et al. Spinal cord stimulation modulates cerebral function: an fMRI study. *Neuroradiology* 2012;54:1399–1407.

8. De Ridder D, Vanneste S. Burst and tonic spinal cord stimulation: different and common brain mechanisms. *Neuromodulation* 2016;19:47–59.

9. Kishima H, Saitoh Y, Oshino S et al. Modulation of neuronal activity after spinal cord stimulation for neuropathic pain; H(2)15O PET study. *NeuroImage* 2010;49:2564–2569.

10. Nagamachi S, Fujita S, Nishii R et al. Alteration of regional cerebral blood flow in patients with chronic pain--evaluation before and after epidural spinal cord stimulation. *Ann Nucl Med* 2006;20:303–310.

11. Shehzad Z, Kelly AM, Reiss PT et al. The resting brain: unconstrained yet reliable. *Cereb Cortex* 2009;19:2209–2229.

12. Apkarian AV. *The brain adapting with pain: contribution of neuroimaging technology to pain mechanisms*. The Netherlands: IASP Press, 2015.

13. Kregel J, Meeus M, Malfliet A et al. Structural and functional brain abnormalities in chronic low back pain: a systematic review. *Semin Arthritis Rheum* 2015;45:229–237.

14. Kolesar TA, Bilevicius E, Kornelsen J. Salience, central executive, and sensorimotor network functional connectivity alterations in failed back surgery syndrome. *Scand J Pain* 2017;16:10–14.

15. Desmond JE, Glover GH. Estimating sample size in functional MRI (fMRI) neuroimaging studies: Statistical power analyses. *J Neurosci Methods* 2002;118:115–128.

16. Behzadi Y, Restom K, Liau J, Liu TT. A component based noise correction method (CompCor) for BOLD and perfusion based fMRI. *NeuroImage* 2007;37:90–101.

17. Power JD, Barnes KA, Snyder AZ, Schlaggar BL, Petersen SE. Spurious but systematic correlations in functional connectivity MRI networks arise from subject motion. *NeuroImage* 2012;59:2142–2154.

18. Whitfield-Gabrieli S, Nieto-Castanon A. Conn: a functional connectivity toolbox for correlated and anticorrelated brain networks. *Brain Connect* 2012;2:125–141.

19. Deogaonkar M, Sharma M, Oluigbo C et al. Spinal cord stimulation (SCS) and functional magnetic resonance imaging (fMRI): modulation of cortical connectivity with therapeutic SCS. *Neuromodulation* 2016;19:142–153.

20. Fair DA, Cohen AL, Power JD et al. Functional brain networks develop from a "local to distributed" organization. *PLoS Comput Biol* 2009;5:e1000381.

21. Farrar JT, Young JP Jr, LaMoreaux L, Werth JL, Poole RM. Clinical importance of changes in chronic pain intensity measured on an 11-point numerical pain rating scale. *Pain* 2001;94:149–158.

22. Hughes CM, McCullough CA, Bradbury I et al. Acupuncture and reflexology for insomnia: A feasibility study. *Acupunct Med* 2009;27:163–168.

23. Eadie J, van de Water AT, Lonsdale C et al. Physiotherapy for sleep disturbance in people with chronic low back pain: results of a feasibility randomized controlled trial. *Arch Phys Med Rehabil* 2013;94:2083–2092.

24. Neblett R, Cohen H, Choi Y et al. The central sensitization inventory (CSI): Establishing clinically significant values for identifying central sensitivity syndromes in an outpatient chronic pain sample. *J Pain* 2013;14:438–445.

25. Osman A, Barrios FX, Kopper BA, Hauptmann W, Jones J, O'Neill E. Factor structure, reliability, and validity of the pain catastrophizing scale. *J Behav Med* 1997;20:589–605.

26. Simes RJ. An improved Bonferroni procedure for multiple tests of significance. *Biometrika* 1986;73:751–754.

27. Sullivan MJ, Stanish W, Waite H, Sullivan M, Tripp DA. Catastrophizing, pain, and disability in patients with soft-tissue injuries. *Pain* 1998;77:253–260.

28. Farrar JT, Pritchett YL, Robinson M, Prakash A, Chappell A. The clinical importance of changes in the 0 to 10 numeric rating scale for worst, least, and average pain intensity: analyses of data from clinical trials of duloxetine in pain disorders. *J Pain* 2010;11:109–118.

29. Farrar JT. What is clinically meaningful: outcome measures in pain clinical trials. *Clin J Pain* 2000;16:S106–S112.

30. Kilgore KL, Bhadra N. Nerve conduction block utilising high-frequency alternating current. *Med Biol Eng Comput* 2004;42:394–406.

31. Kilgore KL, Bhadra N. Reversible nerve conduction block using kilohertz frequency alternating current. *Neuromodulation* 2014;17:242–254. discussion 54-5.

32. Song Z, Viisanen H, Meyerson BA, Pertovaara A, Linderoth B. Efficacy of kilohertz-frequency and conventional spinal cord stimulation in rat models of different pain conditions. *Neuromodulation* 2014;17:226–234. discussion 34-5.

33. Rubinstein JT, Wilson BS, Finley CC, Abbas PJ. Pseudospontaneous activity: stochastic independence of auditory nerve fibers with electrical stimulation. *Hear Res* 1999;127:108–118.

34. Litvak LM, Smith ZM, Delgutte B, Eddington DK. Desynchronization of electrically evoked auditory-nerve activity by high-frequency pulse trains of long duration. *J Acoust Soc Am* 2003;114:2066–2078.

35. Reilly JP, Freeman VT, Larkin WD. Sensory effects of transient electrical stimulation--evaluation with a neuroelectric model. *IEEE Trans Biomed Eng* 1985;32:1001–1011.

36. Lempka SF, McIntyre CC, Kilgore KL, Machado AG. Computational analysis of kilohertz frequency spinal cord stimulation for chronic pain management. *Anesthesiology* 2015;122:1362–1376.

37. Arle JE, Mei L, Carlson KW, Shils JL. High-frequency stimulation of dorsal column axons: potential underlying mechanism of Paresthesia-free neuropathic pain relief. *Neuromodulation* 2016;19:385–397.

38. Crosby ND, Janik JJ, Grill WM. Modulation of activity and conduction in single dorsal column axons by kilohertz-frequency spinal cord stimulation. *J Neurophysiol* 2017;117:136–147.

39. Youn Y, Smith H, Morris B, Argoff C, Pilitsis JG. The effect of high-frequency stimulation on sensory thresholds in chronic pain patients. *Stereotact Funct Neurosurg* 2015;93:335–359.

40. Guan Y, Wacnik PW, Yang F et al. Spinal cord stimulation-induced analgesia: electrical stimulation of dorsal column and dorsal roots attenuates dorsal horn neuronal excitability in neuropathic rats. *Anesthesiology* 2010;113:1392–1405.

41. Shechter R, Yang F, Xu Q et al. Conventional and kilohertz-frequency spinal cord stimulation produces intensity- and frequency-dependent inhibition of mechanical hypersensitivity in a rat model of neuropathic pain. *Anesthesiology* 2013;119:422–432.

42. Abejon D, Rueda P, Vallejo R. Threshold evolution as an analysis of the different pulse frequencies in rechargeable systems for spinal cord stimulation. *Neuromodulation* 2016;19:276–282.

43. Song Z, Meyerson BA, Linderoth B. High-frequency (1 kHz) spinal cord stimulation-is pulse shape crucial for the efficacy? A pilot study. *Neuromodulation* 2015;18:714–720.

44. Craig AD. How do you feel--now? The anterior insula and human awareness. *Nat Rev Neurosci* 2009;10:59–70.

45. Kong J, Jensen K, Loiotile R et al. Functional connectivity of the frontoparietal network predicts cognitive modulation of pain. *Pain* 2013;154:459–467.

46. Becerra L, Sava S, Simons LE et al. Intrinsic brain networks normalize with treatment in pediatric complex regional pain syndrome. *Neuroimage Clin* 2014;6:347–369.

47. Hemington KS, Wu Q, Kucyi A, Inman RD, Davis KD. Abnormal cross-network functional connectivity in chronic pain and its association with clinical symptoms. *Brain Struct Funct* 2016;221:4203–4219.

48. Cottam WJ, Iwabuchi SJ, Drabek MM, Reckziegel D, Auer DP. Altered connectivity of the right anterior insula drives the pain connectome changes in chronic knee osteoarthritis. *Pain* 2018;159:929–938.

49. Uy JP, Galvan A. Sleep duration moderates the association between insula activation and risky decisions under stress in adolescents and adults. *Neuropsychologia* 2017;95:119–129.

50. Moulton EA, Schmahmann JD, Becerra L, Borsook D. The cerebellum and pain: passive integrator or active participator? *Brain Res Rev* 2010;65:14–27.

51. Gu X, Gao Z, Wang X et al. Anterior insular cortex is necessary for empathetic pain perception. *Brain* 2012;135:2726–2735.

52. Gu X, Hof PR, Friston KJ, Fan J. Anterior insular cortex and emotional awareness. *J Comp Neurol* 2013;521:3371–3388.

53. Oertel BG, Preibisch C, Wallenhorst T et al. Differential opioid action on sensory and affective cerebral pain processing. *Clin Pharmacol Ther* 2008;83:577–588.

54. Ahmed S, Yearwood T, De Ridder D, Vanneste S. Burst and high frequency stimulation: underlying mechanism of action. *Expert Rev Med Devices* 2018;15:61–70.

55. De Ridder D, Perera S, Vanneste S. Are 10 kHz stimulation and burst stimulation fundamentally the same? *Neuromodulation* 2017;20:650–653.